Phase Transitions in Magneto-Electric Hexaferrites

Tatyana Koutzarova,* Svetoslav Kolev, Kiril Krezhov, and Borislava Georgieva

Cite This: *ACS Omega* 2022, 7, 44485−44494

Read Online

ACCESS | Metrics & More | Article Recommendations

ABSTRACT: Hexaferrites have long been the object of extensive studies because of their great possibility for applications—permanent magnets, high-density recording media, microwave devices, in biomedicine, to name but a few. Lately, many researchers' efforts have been focused on the existence of the magneto-electric effect in some hexaferrite systems and the appealing possibility of them being used as single-phase multiferroic and magneto-electric materials. As indicated by theoretical analyses, the origin of the large magneto-electric effect can be sought in the strong interaction between the magnetization and the electric polarization that coexist in insulators with noncollinear magnetic structures. The hexaferrites' magnetic structure and, particularly, the specific magnetic spin ordering are the key factors in observing magneto-electric phases in hexaferrites. Some of these phases are metastable, which hampers their direct practical use. However, as the

hexaferrites' phase diagrams reveal, chemical doping can be used to prepare a number of noncollinear stable magnetic phases. Since the magneto-electric effect has to do with the magnetic moments ordering, it seems only logical that one should study the cation substitutions' influence on the magnetic phase transition temperature. In this paper, we summarize recent examples of advances in the exploration of magnetic phase transitions in Y-type hexaferrites. In particular, the effect is emphasized by substituting in Y-type hexaferrites the nonmagnetic Me^{2+} cations with magnetic ones and of the magnetic Fe^{3+} cations with nonmagnetic ones on their magnetic properties and magnetic phase transitions. The work deals with the structural properties of and the magnetic phase transitions in a specific Y-type hexaferrite, namely, $Ba(Sr)_2Me_2Fe_{12}O_{22}$.
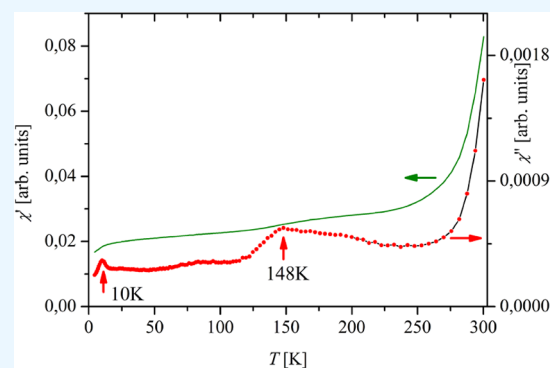
INTRODUCTION

In order for a magneto-electric multiferroic material to become appropriate for practical use, the magneto-electric coupling in it should become active and large at room temperature; i.e., the magnetic ordering temperature should be high. However, ferroelectricity and ferromagnetism coexist in few materials that mostly provide a rather weak ferromagnetism.[1,2] The research has so far been focused mainly on three types of multiferroics—composites containing ferroelectric and ferromagnetic materials, ferroelectric materials doped with metal cations, and ferrites with spiral ordering of the magnetic moments.[3−5] Although over ten systems of different composition have so far been studied comprehensively, a high degree of linking between the magnetic and electric parameters in single-phase materials (especially near room temperature) is still to be found, which hinders their application.

Therefore, preparing a material where large ferroelectricity and strong ferromagnetism take place simultaneously would be a landmark in the progress toward electronic and functionalized materials.[3] As assumed, the large magneto-electric effect arises in insulators with long wavelength cycloidal, sinusoidal, spiral, and conical magnetic structures, where the possibility exists of a strong interaction between magnetization and electric polarization.[4] One type of material with such a structure is the hexaferrites, which are promising multiferroic materials allowing one to control the polarization by way of applying magnetic fields at room temperature.[5−8]

Kimura and co-authors[9] were the first to observe a magneto-electric effect in hexaferrites in a monocrystal of $Ba_{0.5}Sr_{1.5}Zn_2Fe_{12}O_{22}$ (Y-type hexaferrite) in a 1 T magnetic field and close to room temperature, the effect becoming meaningful at $T < 130$ K.[10] Kimura et al.[9] described the existence of the screw structure in the absence of a magnetic field that is incommensurably modulated by weak magnetic fields, three intermediate structures commensurably modulated by a magnetic field, and, last, a ferrimagnetic collinear structure formed at 2.2 T, all accessible at room temperature. Magneto-electric coupling was observed in the intermediate III phase with a $\bar{3}'m$ magnetic symmetry and appeared on the $M-H$ plots as a plateau with a varying slope in the 0.3 T−2.2 T

interval. Within this the magnetic field range, at 10 K, the electric polarization had the maximum value of 150 $\mu C/m^2$.

CRYSTAL AND MAGNETIC STRUCTURE

The Y-hexaferrites' crystalline structure is classified in the rhombohedral space group $R(-3m)$. The unit cell is formed by three formula units ($Z = 3$). The structure is considered as built of two types of crystalline S and T blocks successively stacked along the hexagonal c-axis as (TST'ST"S"), the primes signifying a 120° rotation about the c-axis.[11] Thus, the hexagonal unit cell comprises three T and three S blocks with 18 oxygen layers. There exist four recurrent cubic closely packed oxygen layers that are followed by two barium-containing hexagonal closely packed layers, forming a close packing sequence. The S block ($Me_2Fe_4O_8$; spinel block) can be considered a double spinel layer. It contains two spinel units of two layers of four oxygen atoms with three metal atoms in four octahedral sites between each layer—the cation is surrounded by six oxygen anions and two tetrahedral sites where four oxygen anions enclose the cation.[11] Thus, the metals occupy six sites, four being octahedral and two tetrahedral. The T block ($Ba_2Fe_8O_{14}$) is formed by four oxygen layers, with one oxygen atom being substituted by a barium atom in the inner two layers, which face one another in the neighboring layers; this results in two tetrahedral sites and six octahedral ones.[11] All cations (Me^{2+} and Fe^{3+}) occupy six concrete crystallographic sites: two tetrahedral sites (6_{cIV}, 6_{c*IV}) and four octahedral sites (3_{aVI}, 3_{bVI}, 6_{cVI}, and 18_{hVI}). There are two octahedral sites in the T block and one in the S block; the octahedral site h having the highest multiplicity is common for both the T and S blocks. For example, the Mg^{2+} ions occupy randomly tetrahedral and octahedral sites in $Ba_2Mg_2Fe_{12}O_{22}$,[12] whereas the Zn^{2+} cations would rather be positioned in tetrahedral sites as the Fe^{3+} cations.[13] To understand and design the magnetic and other physical properties, it is necessary to have information on the material's crystalline structure, on the ions' distributions, and on the interactions between the cations occupying different sites. The earliest considerations regarding the possible spin arrangement in the Y-type hexaferrite structure date as far back as the 1950s.[14]

Using a qualitative methodology and the available magnetic data, Gorter[15] was able to predict the magnetic moments' orientation in the Y-type ferrite sublattices, together with the superexchange interactions' relative strength. The c-axis is normal to the plane where the easy magnetization axis lies, while the dominating majority spins in octahedral 3a, 3b, and 18h sites, and the minority spins in tetrahedral $6c_T$ and $6c_S$ and octahedral 6c sites give rise to the uncompensated magnetic moment lying in the ab-plane. The majority and minority spins define two magnetic sublattices that differ from the blocks of the crystalline structure: L_m blocks (spins in octahedral 3a, 3b, and 18h sites) and S_m blocks (spins in tetrahedral $6c_T$ and $6c_S$ and octahedral 6c sites) alternating along [001] and bearing opposite large and small magnetization, respectively.[12] The existence of these two sublattices (L_m and S_m) is in the origin of the Y-type hexaferrites' magnetic behavior, i.e., of the strongest magnetic interaction occurring within the T block. The superexchange interaction crossing the sublattices boundaries, Fe(4)—O(2)—Fe(5), can be impacted by a suitable substitution. Thus, in the Y-type hexaferrites, the T block, the one containing the Fe(4)—O(2)—Fe(5) bonds, is essential in giving rise to the noncollinear screw structure.

The magnetic phase transitions in single-crystal Y-type hexaferrites have been comprehensively studied in the cases of $Ba_2Mg_2Fe_{12}O_{22}$[16] and $Sr_{1.5}Ba_{0.5}Zn_2Fe_{12}O_{22}$,[17,18] which revealed the considerable complexity of the magnetic phase diagram. The significance was observed of not only the metal cations' crystallographic positions but also of the crystal lattice defects, such as of oxygen at the crystalline surface. Typically, two transitions occur, from ferromagnetic collinear to proper screw (helical) magnetic moments ordering and from proper screw to a conical one. For monocrystal $Ba_2Mg_2Fe_{12}O_{22}$, these two magnetic phase transformations occur at 195 and 50 K, respectively.[10] The magnetic moments of the L_m and S_m blocks in the proper screw phase rotate around the c-axis.[12] The slanted conical spin ordering arises after a magnetic field of 30 mT is applied at temperatures below 195 K.[4] The conical spin angle can be changed by varying the temperature and the applied magnetic field. $Ba_2Mg_2Fe_{12}O_{22}$ acquires a collinear ferrimagnetic ordering with the opposite directions of the L_m and S_m blocks in the ab-plane above 195 K up to 553 K.[4,10] Figure 1 illustrates the changing spin ordering for these phase transitions; more detail can be found in ref 19.
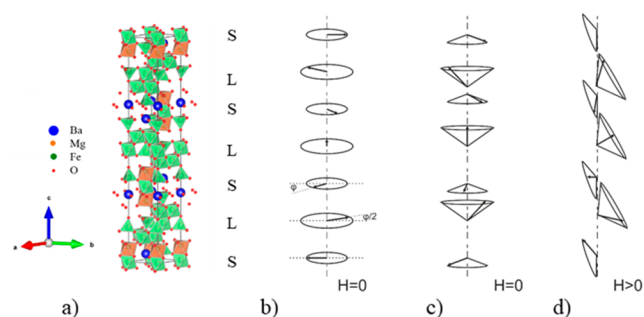

Figure 1. Schematic crystal structure of $Ba_2Mg_2Fe_{12}O_{22}$ (a). Illustrations of helicoidal spins with (b) proper screw, (c) longitudinal conical, and (d) slanted conical spin arrangements.

It is well-known that $Ba_{0.5}Sr_{1.5}Zn_2Fe_{12}O_{22}$ exhibits a helical spin ordering, which below 326 K (Néel temperature) is characterized by the spin moments lying and rotating in the ab-plane.[18] This results from the fact that the Ba^{2+} cations' partial substitution by Sr^{2+} cations in $Ba_{2-x}Sr_xZn_2Fe_{12}O_{22}$ distorts the lattice around the Sr^{2+} positions because of the strontium's smaller ionic radius and Zn^{2+} and Fe^{3+} being redistributed to tetrahedral sites. The turn angle is between 0° and 180° for 1 < x < 1.6, leading to the helical spin ordering. Detailed descriptions of the crystal and magnetic structures were given by Momozawa et al.[17] Applying a magnetic field normally to the c-axis induces different intermediate magnetic phases forming a slightly modified helix at low field to a collinear ferromagnetic phase at high field. The magnetic cation environment plays a key role not only in the genesis of the magnetic properties but also of the magneto-electric effect; moreover, understanding the metal cations influence on the structural changes on a crystal cell level is of particular significance.

SYNTHESIS TECHNIQUES OF Y-TYPE HEXAFERRITES

The research aimed at elucidating the magneto-electric effect's origin in hexaferrites has mostly been conducted on monocrystal samples; however, for possible applications,

novel data should be acquired on this effect in polycrystalline materials and in thick and thin films. Obtaining monophase samples of Y-hexaferrites presents several obstacles, which is why one usually finds in the literature information on the magneto-electric effect in monocrystals. As has been found, the intervals of temperatures allowing synthesis of hexaferrites' different phases, namely, the M-, Y-, Z-, W-, and U-types, overlap;[11,14] i.e., the different hexaferrite-type structures may coexist in a certain temperature interval. Clearly, synthesizing monophase samples is not an ordinary task. Their preparation route entails the coexistence of different magnetic oxides, mainly because usually the temperature range leading to their formation is very narrow, as especially clearly manifested in the synthesis of the Y phase. Zhuravlev et al.[20] summarized their findings on the phase composition of samples from the $Ba_2Ni_{2-x}Cu_xFe_{12}O_{22}$ system synthesized by the classical ceramic technology. Pullar[11] presented an extensive overview on the influence of the synthesis conditions of the classical ceramic technology on the production of the different hexaferrite types. The M-type hexaferrite, which has the simplest crystalline structure of all the hexaferrite family, starts to appear at 900 °C as a minor phase and is the main phase in the range of 800−1200 °C. This indicates that the M-type hexaferrite is always present during the synthesis of the other hexaferrite types in this temperature range. Ordinarily, the Y phase synthesis starts at 900 °C; in the temperature range of 900−1200 °C, it is the main phase together with the M-type phase.[11] Thus, preparing the Y-type hexaferrite begins at 900 °C and entails the existence of another hexaferrite type, namely, M-type barium hexaferrite, as well as of second phases of hexagonal barium ferrite and of spinel ferrites, both in small amounts. At this temperature, the M-type hexaferrite phase dominates. The Y-type phase amount increases with the temperature and is predominant at 1100 °C. A Z-type hexaferrite appears at temperatures above 1150 °C, so that the three types of hexaferrite phases coexist in the range of 1150−1250 °C, while the Z-type phase becomes dominant above 1200 °C. With a further temperature increase, the amount of the Y-type hexaferrite phase decreases, and at 1300 °C, it is a secondary product of the synthesis. The concomitant second phase type depends to a large degree on the Me cation type and on the method of preparation. To overcome the problem of the different hexaferrite structural types coexisting, researchers have resorted to using nonstoichiometric mixtures of oxides and $BaCO_3$, changing the precursors, rapid cooling at high temperature, or using other synthesis methods, most of which are modified "wet chemistry" pathways. With this in mind, the existence of minor phases that can affect the multiferroic parameters of the material must be taken into account when examining Y-type hexaferrite. Below, we present the most widely used methods of Y-type hexaferrite synthesis.

Classical Ceramic Technology. The classical ceramic technology is the most popular method for preparation of complex polycrystalline oxides. A large amount of research effort has been focused on the preparation of single-phase Y-type hexaferrites.[21−26] In summary, the technique is based on a solid-state reaction of alkaline earth carbonates with metal oxides. The powders are homogenized by ball-milling and, after palletization, are synthesized at a high temperature in the 1100−1200 °C range to obtain single-phase Y-type hexaferrite. Rhee et al.[27] synthesized $Ba_2Co_2Fe_{12}O_{22}$ at 1200 °C in an oxygen atmosphere to reduce the number of oxygen defects. The samples produced have particle sizes from a few to ten

microns.[28,29] Although the solid-state reaction route is simple and accessible, the large particle size and the homogeneity of the final product can be a problem for certain applications; also, the temperatures required to complete the reaction are usually high, which may be inconvenient for a later large-scale reproducible production.

Sol−Gel Autocombustion Method. A popular method for producing hexaferrites is the sol−gel autocombustion, with citric acid often used as fuel and chelator.[30−32] The synthesis procedure is as follows: as starting materials, the respective metal nitrates are used; citric acid solution is carefully added to form stable complexes with the metal cations and prevent their precipitation in the solution. As the metal citrates are stable without precipitation at pH = 7−8, an ammonia solution is usually added. The solution is slowly evaporated to form a gel, which is dehydrated at 120 °C. During the dehydration, the gel turns into a fluffy mass and combusts in a self-propagating way. The autocombustion is an exothermic reaction of oxidation−reduction, with the heat discharged sufficing to form an oxide mixture. The autocombusted material thus prepared is usually heat-treated at temperatures below 850 °C to eliminate the remaining organic precursors. The final calcination is carried out in the temperature range between 900 and 1200 °C depending on the specific Y-hexaferrite. Figure 2a displays the
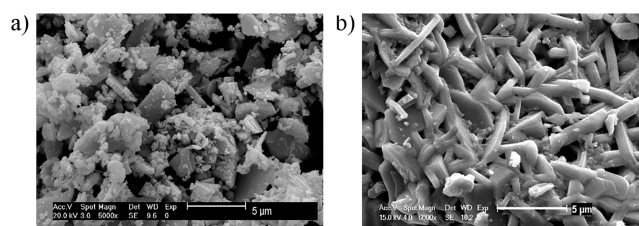

Figure 2. SEM image of $Ba_2Mg_2Fe_{12}O_{22}$ powders prepared via (a) autocombustion[33] and (b) ultrasonically assisted co-precipitation.[35] (a) Reprinted with permission from ref 33. Copyright 2012 Springer. (b) Reprinted with permission from ref 35. Copyright 2017 IEEE.

morphology of $Ba_2Mg_2Fe_{12}O_{22}$ powders.[33] As seen, the particles have agglomerated well and have formed clusters of various sizes and shapes, with some clusters having a plate-like shape. Such a considerable degree of aggregation is the result of the strong magnetic attraction forces. The sol−gel autocombustion methods allow the synthesis of powders with a particle size of less than 1 μm and a narrow size distribution; i.e., they provide an ability to control the microstructure. For example, Ahmad et al.[34] produced $Sr_2Ni_{2-x}Mg_xFe_{12}O_{22}$ samples with an average grain size of 0.74−1.01 μm. The narrow size distribution is important for possible future application of the powder obtained. As a "wet chemistry" and a multistage method, the sol−gel autocombustion synthesis allows a large number of modifications to be made to improve the quality of the Y-type hexaferrite powders.

In ref 36, Koutzarova et al. presented a study on the formation of Ni-doped $Ba_2Zn_2Fe_{12}O_{22}$. The synthesized specimens were a spinel-type Ni−Zn mixed ferrite $(Zn,Ni)-Fe_2O_4$ with the crystallites size ranging from 10 to 12 nm. The second crystal phase was a mixed barium−strontium carbonate, $(Ba,Sr)CO_3$, with crystallite sizes within the 18−19 nm interval. The heat treatment at 800 °C resulted in the carbonate constituent vanishing and Ba−Sr oxides being formed, namely, $BaFeO_{3-x}$ and $BaSrFe_4O_8$.

Co-precipitation and Ultrasonically Assisted Co-precipitation Methods. Still another regularly applied technique of synthesizing magnetic oxides is co-precipitation. The starting materials are usually metal nitrates or metal chlorides.[37,38] The co-precipitation process occurs upon adding alkali hydroxide at appropriate pH, usually between 11 and 12.5. Hsiang and Yao investigated the formation of $Ba_2Co_2Fe_{12}O_{22}$ and found that it was obtained through a $BaFe_{12}O_{19}$ (M-type hexaferrite) and $BaFe_2O_4$ reaction.[39] Lehlooh et al.[40] studied the co-precipitation process conditions and the annealing temperature during the synthesis of $Ba_2Co_2Fe_{12}O_{22}$. They found that when the co-precipitation was carried out at pH = 10 and the precipitating agent (NaOH + Na_2CO_3) was added dropwise, single-phase Y-type hexaferrite could be obtained in the temperature range of 1000−1100 °C. When the co-precipitation occurred at pH = 14 and the precipitation agent was added quickly, a pure of $Ba_2Co_2Fe_{12}O_{22}$ phase could not be produced. We discuss also a modification of the method, namely, the ultrasonically assisted co-precipitation, whereby the metal cations' co-precipitation is started by addition of NaOH at pH = 11.5−12 during the action of an ultrasound wave at high power. Within a short period of time, the temperature and pressure increase up to, respectively, 5000 K and 800 atm. Bubbles are generated, which grow and then implode, thus enhancing the rate of reaction, the mass transport, and the heat effects. The precursors produced by these co-precipitation methods are synthesized at 1170 °C. We described in detail such a procedure for the synthesis of different Y-type hexaferrites.[41−44] We also reported[35,41] a comparative investigation on this synthesis method's effect on the microstructural and magnetic parameters of $Ba_2Mg_2Fe_{12}O_{22}$ powder materials and found that the ultrasonically assisted co-precipitation produced particles with a practically perfect hexagonal shape compared with the particles obtained by sol−gel autocombustion (Figure 2b). The average thickness of the $Ba_2Mg_2Fe_{12}O_{22}$ particles was 380 nm. A similar microstructure was observed for $Ba_{0.5}Sr_{1.5}Zn_2Fe_{12}O_{22}$.[43,44]

We should note that the process of preparation is not the only factor affecting the powders' microstructure; the latter changes upon substituting the metal cations, as well. For example, in the studies on the effect of Al substitution in the $Ba_{0.5}Sr_{1.5}Zn_2Fe_{12}O_{22}$ hexaferrite system, a melting process was observed to take place during the synthesis of the substituted $Ba_{0.5}Sr_{1.5}Zn_2Al_{0.08}Fe_{11.92}O_{22}$ hexaferrite by sol−gel autocombustion (Figure 3).[45]

MAGNETIC PROPERTIES OF Y-HEXAFERRITES

The Y-type hexaferrites possess an easy axis lying in the basal *ab*-plane, which is why the hysteresis curves are very narrow;
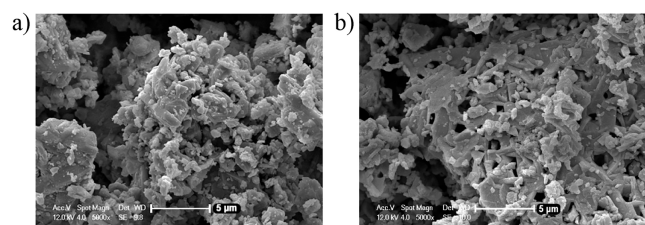

Figure 3. SEM images of (a) $Ba_{0.5}Sr_{1.5}Zn_2Fe_{12}O_{22}$ powders and (b) $Ba_{0.5}Sr_{1.5}Zn_2Al_{0.08}Fe_{11.92}O_{22}$ powders prepared by autocombustion.[45] Reprinted with permission from ref 45. Copyright 2018 Springer.

i.e., they are very soft magnets (with a low coercivity, H_c). Most the ferrites of Y type are hexaplane ferrites, meaning that they have a simple magnetization plane normal to the *c*-axis or an easy-magnetization cone at room temperature. The $Ba_2Cu_2Fe_{12}O_{22}$ is the only Y-type hexaferrite that has so far been observed to possess a preferred uniaxial direction of magnetization. The saturation magnetization (M_s) value is between 20 and 40 emu/g, with H_c being from a few oersteds to 200 Oe at room temperature. The metal cation type and the Ba:Sr ratio in $Sr_xBa_{2−x}Me_2Fe_{12}O_{22}$ play a major role in determining these values. Gao et al.[29] showed that the annealing temperature for synthesis of $Ba_2Co_2Fe_{12}O_{22}$ powder affects the H_c value. Fujii et al.[46] found that in the case of $Ba_2ZnCuFe_{12}O_{22}$ the synthesis temperature does not impact significantly the saturation magnetization, while the coercive field decreases from 52.6 to 2.7 Oe as the temperature of sintering is raised from 900 °C to 1200 °C.

In the Y-type hexaferrites exhibiting the magnetoelectric effect, a triple hysteresis curve is very often manifested, revealing the presence of two magnetic states in the sample. Such a curve at room temperature is shown in Figure 4a for
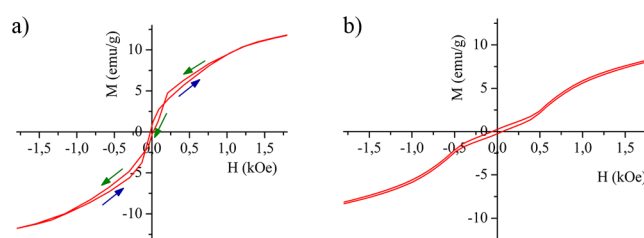

Figure 4. Hysteresis curves in the low magnetic field range of $Sr_{1.5}Ba_{0.5}Zn_2Fe_{11.92}Al_{0.08}O_{22}$ powder synthesized by (a) ultrasonically assisted co-precipitation[43] and (b) sol−gel autocombustion.[31] (a) Reprinted with permission from ref 43. Copyright 2016 Bulgarian Chemical Communications. (b) Reprinted with permission from ref 31. Copyright 2021 IOP Conference Series.

samples of $Sr_{1.5}Ba_{0.5}Zn_2Fe_{11.92}Al_{0.08}O_{22}$ obtained by ultrasonically assisted co-precipitation.[43] The appearance of a triple hysteresis loop in the range of weak magnetic fields between 1 kOe and −1 kOe points to the existence of an intermediate phase between the proper screw spin phase and the collinear ferromagnetic one.

Similar behavior was also observed for $SrBaMg_2Fe_{12}O_{22}$ and $Sr_{1.5}Ba_{0.5}Mg_2Fe_{12}O_{22}$ at room temperature,[47] $BaSrMg_2Fe_{11.48}Mn_{0.52}O_{22}$ at 5 K,[22] and for $Ba_{0.5}Sr_{1.5}Zn_{2−x}Ni_xFe_{12}O_{22}$ at 4.2 K.[36] Figure 4b presents the difference in the hysteresis loop behavior at 300 K in the weak magnetic fields range for a $Ba_{0.5}Sr_{1.5}Zn_2Al_{0.08}Fe_{11.92}O_{22}$ sample obtained by sol−gel autocombustion; as seen, a triple hysteresis curve is not observed.[31] This points to the existence of two types of ferromagnetic states with different ordering of the magnetic moments. As it is in the range of weak magnetic fields, this could be related to a ferrimagnetic and a helical ordering of spins. Such a behavior was again observed for $Ba_{0.5}Sr_{1.5}Zn_{0.5}Ni_{1.5}Fe_{11.92}Al_{0.08}O_{22}$[32] and $Ba_{0.5}Sr_{1.5}NiMgFe_{12}O_{22}$[48] powders. It is well-known that in $Ba_{2−x}Sr_xZn_2Fe_{12}O_{22}$, substituting Sr^{2+} at $x = 1.5$ causes a magnetic phase change from a ferromagnetic Fe^{3+} spin order in the nonsubstituted samples to a screw spin ordering.[17,49] Once impacted by a weak magnetic field, the magnetic system experiences transformations via metamagnetic states, including

such between screw spin ordering and conical spin ordering. These magnetic structure alterations influence the specimen's magnetization and bring about the appearance of a multistage hysteresis loop.

MAGNETIC PHASE TRANSITIONS

The magnetic phase transitions can be provoked by a temperature change and/or by a change in the applied magnetic field. The magnetic field-dependent phase transitions are manifested by a change in the course of the initial magnetization curve at a constant temperature and an increasing dc magnetic field. This kind of magnetization curve behavior is strongly expressed in single crystals, whereas in polycrystalline samples, these effects are less pronounced due to the influence of the size and the direction of magnetization of the individual particles. Georgieva et al.[31] studied the initial magnetization of a $Ba_{0.5}Sr_{1.5}Zn_2Al_{0.08}Fe_{11.92}O_{22}$ powder sample; changes were seen in the $M(H)$ curve slope at 4.2 K for magnetic fields in the range of 5−20 kOe. These result from occurring metamagnetic transitions and to intermediate phases with different conical magnetic moments ordering in the crystal lattice. A similar step-like behavior was reported in ref [48] for $Ba_{0.5}Sr_{1.5}NiMgFe_{12}O_{22}$ powders also at 4.2 K. In ref [29], magnetic phase transitions were reported at 1.9 kOe, 8.5 kOe, and 20 kOe, corresponding to three ferroelectric phases and one ferromagnetic phase with collinear spins above 20 kOe in $BaSrCoZnFe_{11}O_{22}$ polycrystalline samples at 200 K. In ref [50], a step-like behavior was registered in the initial magnetization curves of polycrystalline $Ba_{0.5}Sr_{1.5}Zn_{2-x}Mg_xFe_{12}O_{22}$ samples (x = 0−2), indicating that the increasing magnetic field induces intermediate magnetic phases ranging from conical ferromagnetic to proper screw spin orderings. The authors further[51] observed an analogous magnetization curve variation for polycrystalline samples of $Ba_{0.5}Sr_{1.5}Zn_{2-x}Mg_xFe_{11}AlO_{22}$, but for $x \geq 0.8$. Kim et al.[52] explored the magnetic parameters of the $Ba_{2-x}Sr_xNi_2(Fe_{1-y}Al_y)_{12}O_{22}$ system and observed a step-like behavior in the initial magnetization plot at 295 K only for the $Ba_{0.5}Sr_{1.5}Ni_2(Fe_{0.97}Al_{0.03})_{12}O_{22}$ sample corresponding to the magnetic phase transition related to the conical spin state. Abdullah et al.[21] observed a step-like behavior at 5 K and a lower magnetic field in $Ba_2Mg_2(Fe_{1-x}Mn_x)_{12}O_{22}$ powders. At magnetic fields above 400 Oe, the $Ba_2Mg_2(Fe_{1-x}Mn_x)_{12}O_{22}$ powders exhibit few intermediate phases (I, II, and III) and a collinear ferrimagnetic phase at magnetic fields near 22 kOe.

We turn our attention now to the investigations of the magnetic phase transitions induced by temperature changes under an applied external (constant or alternating) magnetic field. For a constant external magnetic field, the changes in the magnetization curve with the temperature is monitored by carrying out the measurements following a zero-field-cooled (ZFC) and a field-cooled (FC) protocol. We will briefly present and compare the major results of our studies on the ZFC magnetization in a 100 Oe magnetic field of samples of $Ba_2Mg_2Fe_{12}O_{22}$ powders produced by sonochemical co-precipitation and by sol−gel autocombustion. The changes in both temperature dependencies indicating phase transitions take place in the vicinity of 183 and 40 K. The low-temperature phase transition from a helical to a conical spin ordering is more clearly observed in the samples prepared by sonochemical co-precipitation due to the development of large particles of a well-defined hexagonal shape when this techniques is used. Rhee et al.[27] investigated the ZFC

magnetization changes for $Ba_2Co_2Fe_{12}O_{22}$ in a magnetic field of 100 Oe; they observed the magnetic phase transition from a helimagnetic spin ordering to a ferromagnetic one to take place at 215 K and determined the T_N to be 615 K. The Néel temperature is higher than that for $Ba_2Mg_2Fe_{12}O_{22}$ and $Ba_2Zn_2Fe_{12}O_{22}$ due to the presence of the magnetic Co^{2+} cation leading to stronger superexchange interactions $Co^{2+}-O^{2-}-Fe^{3+}$ (Co^{2+}). Lim et al.[53] studied the ZFC magnetization of $Ba_2Mg_{0.5}Co_{1.5}Fe_{12}O_{22}$ in the 50−740 K temperature interval and a magnetic field of 100 Oe and detected a magnetic phase transition from a helimagnetic spin ordering to a ferromagnetic one at 206 K. Our studies[42] on the influence of the partial substitution of nonmagnetic Mg^{2+} cations with magnetic Co^{2+} cations in $Ba_2Mg_{0.4}Co_{1.6}Fe_{12}O_{22}$ showed that the phase transition temperature is rather sensitive to the applied magnetic field strength, namely, it decreases from 225 K (at 50 Oe) to 135 K (at 1 kOe). We also observed a different behavior of the ZFC curves for magnetic field strengths exceeding 500 Oe. The ZFC curves start decreasing upon reaching the helical ferrimagnetic phase transition and overlapping of the ZFC and FC curves occurs around 285 K. Kim and co-workers[54] showed that the temperature of a magnetic phase transition from helimagnetic spin ordering to ferromagnetic one in $Ba_2CoZnFe_{12}O_{22}$ decreased from 200 to 115 K when the magnetic Co^{2+} cations were half-substituted by the nonmagnetic Zn^{2+} cations. A detailed investigation of this phase transition for the $Ba_2Co_{2-x}Zn_xFe_{12}O_{22}$ system was reported in ref [55], but the second phase transformation from a helical to a longitudinal conical magnetic moments ordering was not seen in the entire (x = 0−2) range. Behera and Ravi[56] also investigated the effect of substitution with Zn^{2+} on the helical ferrimagnetic phase transformation in $Ba_2Co_{2-x}Zn_xFe_{12}O_{22}$ in the same range of substitution for powders obtained by a solid-state technique. The helical ferrimagnetic phase transition temperature decreased from 225 K for x = 0 to around 60 K for x = 1.5. They did not observe a second phase transition from a helical to a longitudinal conical spin ordering for a sample of $Ba_2Zn_2Fe_{12}O_{22}$. In another study,[57] the authors found that the transition to a helicoidal spin order shifted to a lower temperature due to the decreasing magnetic anisotropy as the Mg^{2+} cation concentration in $Ba_2Co_{2-x}Mg_xFe_{12}O_{22}$ was raised in the range of x = 0−0.5. The conical transition was also not observed for Mg-substituted $Ba_2Co_2Fe_{12}O_{22}$. Wang et al.[28] observed a sharp peak in the ZFC and FC magnetization curves at 365 K in $BaSrCoZnFe_{11}O_{22}$ and attributed it to the corresponding collinear ferromagnetic spiral spin magnetic phase transition in single-crystalline sample.

The substitution of Fe^{3+} with the smaller Al^{3+} gives rise to a possibility of changing not only the crystal cell parameters with the resulting alteration of the Fe(4)−O(2)−Fe(5) bonds but also the magnetic ordering, since the Al^{3+} cation is non-magnetic and prefers to take the octahedral site with up-spin related to the 3a, 3b, and 18h sites. Below, we present results from investigating the influence of the amount of Al^{3+} substitution on the magnetic phase transition in $Ba_{0.5}Sr_{1.5}Zn_2Fe_{12-x}Al_xO_{22}$.

Xu et al.[30] followed the phase transitions in $Ba_{0.5}Sr_{1.5}Zn_2Fe_{11.52}Al_{0.48}O_{22}$ bulk samples by measuring the ZFC and FC magnetization in the 5−800 K temperature interval in an applied magnetic field of 100 Oe. They observed a magnetic phase transition from a longitudinal conical spin phase to a proper screw spin phase at 25 K and from a proper
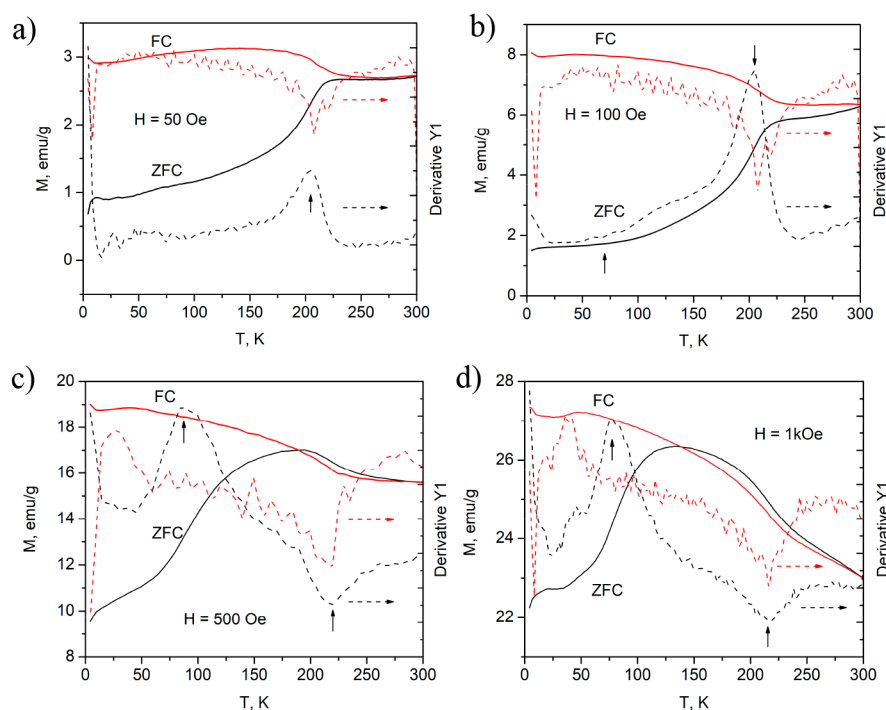
Figure 5. ZFC and FC magnetization as a function of the temperature for $Ba_2Mg_{0.4}Co_{1.6}Fe_{12}O_{22}$ in a magnetic field of (a) 50 Oe, (b) 100 Oe, (c) 500 Oe, and (d) 1 kOe. Reprinted with permission from ref 42. Copyright 2019 MDPI.

screw spin phase to a ferromagnetic spin phase at 297 K. They also observed two-step changes in the ZFC magnetization curve at 400 and 600 K that they associated with an intermediate phase between a proper screw and a ferromagnetic spin ordering. Investigating the magnetic behavior of the $Ba_{2-x}Sr_xNi_2(Fe_{1-y}Al_y)_{12}O_{22}$ system at a magnetic field of 100 Oe (ZFC magnetization measurements), Kim et al.[52] found that the temperature of the magnetic structure change from helical to ferrimagnetic ordering increased with Sr and Al ions substitutions, e.g., from 47 K to room temperature for $Ba_{0.5}Sr_{1.5}Ni_2(Fe_{0.97}Al_{0.03})_{12}O_{22}$ (Figure 5).

In ref 31, the dependence on the temperature was followed of the ZFC and FC magnetization plots of the $Ba_{0.5}Sr_{1.5}Zn_2Al_{0.08}Fe_{11.92}O_{22}$ polycrystalline powder under magnetic fields of 50, 100, and 500 Oe in the 4.2−300 K temperature interval. It was shown that the magnetization is reduced slowly to about 285 K and begins growing with the temperature being raised to exceed 300 K, which is related to a magnetic transformation from a collinear ferrimagnetic to a proper screw spin phase. It was also shown that the ZFC and FC magnetization curves' behavior in a 500 Oe magnetic field differs significantly from that at weak fields; thus, the well-defined peak at 95 K can be regarded as pointing to a longitudinal conical magnetic moments ordering established under this temperature.

In the case of $Ba_{0.5}Sr_{1.5}Co_2Fe_{12}O_{22}$, a magnetic phase transition to longitudinal conical spin ordering below 255 K in a magnetic field of 100 Oe was reported by Wang et al.[58] In addition, they observed an intermediate phase, namely, a mixed helical and collinear spin ordering in the temperature range of 255−310 K under the same magnetic field.

By measuring the ZFC magnetization at H = 100 Oe,[50,51] the effect was studied of substituting the Zn^{2+} cation by Mg^{2+} cations in $Ba_{0.5}Sr_{1.5}Zn_{2-x}Mg_xFe_{12}O_{22}$ and $Ba_{0.5}Sr_{1.5}Zn_{2-x}Mg_xFe_{11}AlO_{22}$ (x = 0−2) on the magnetic

phase transitions. Raising the temperature, the authors detected two phase transitions—from a longitudinal conical to a proper screw magnetic moments arrangement and from a proper screw to a collinear ferromagnetic phase. They also found that by increasing the Mg^{2+} concentration up to x = 1.2 in $Ba_{0.5}Sr_{1.5}Zn_{2-x}Mg_xFe_{11}AlO_{22}$, the temperatures of these two magnetic phase transitions can be raised, due to the stronger superexchange interaction.[51] The samples of $Ba_{0.5}Sr_{1.5}Zn_{2-x}Mg_xFe_{12}O_{22}$ exhibited a proper screw to a collinear ferromagnetic phase transition above room temperature.[50] In our earlier study on $Ba_{0.5}Sr_{1.5}NiMgFe_{11}AlO_{22}$,[48] we showed that a gradual decrease is initiated of the FC magnetization at a temperature close to 38 K; however, at about 150 K, the tendency is reversed to a monotonic rise, while the ZFC magnetization also rises as the temperature is raised. The maximum visible at 70 K has to do with the intermediate magnetic phase transformation. Another maximum at 40 K is also observed—it originates from the magnetic phase transition from a spiral magnetic ordering to a conical spin ordering at low temperatures.

Abdullah et al.[22] investigated the Sr substitution effect in the $Ba_{2-x}Sr_xMg_2Fe_{11.48}Mn_{0.52}O_{22}$ ($0 < x \leq 1$) hexaferrite and found that the Sr substitution raises the spin ordering transition temperature from a proper screw state to a longitudinal conical spin state from 52 to 73 K and from a ferrimagnetic state to a proper screw state, from 210 to 315 K in a 100 Oe magnetic field. In another study,[21] they found that Mn doping at Fe sites raises the transformation temperature from a ferrimagnetic state to a proper screw state from 190 to 208 K, while a drop was seen in the proper screw to longitudinal conical spin transformation temperature from 35 to 25 K in $Ba_2Mg_2(Fe_{1-x}Mn_x)_{12}O_{22}$ in a magnetic field of 100 Oe.

In a further attempt to clarify the magnetic changes in hexaferrite samples, we will next discuss another type of measurement that is related with the dependence of the
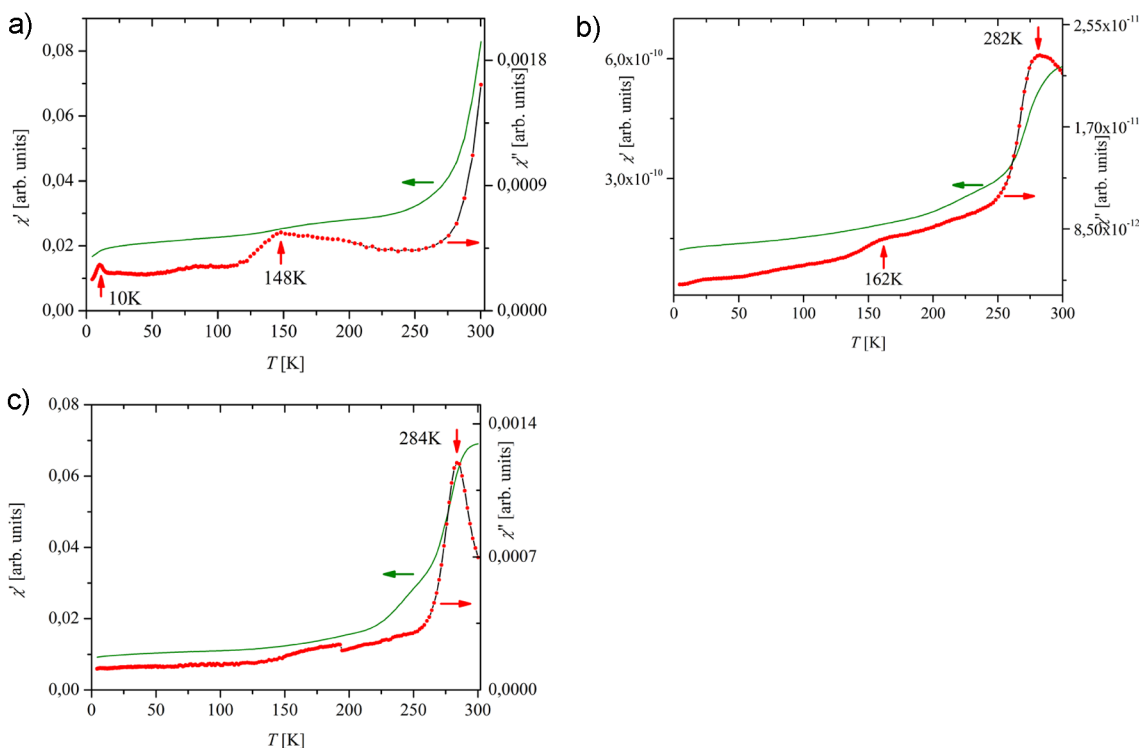
Figure 6. Differential ac susceptibility (real part χ' and imaginary part χ'') as a function of the temperature for samples (a) $Ba_{0.5}Sr_{1.5}Zn_{1.2}Ni_{0.8}Fe_{12}O_{22}$, (b) $Ba_{0.5}Sr_{1.5}ZnNiFe_{12}O_{22}$, and (c) $Ba_{0.5}Sr_{1.5}Zn_{0.5}Ni_{1.5}Fe_{12}O_{22}$ recorded in an ac magnetic field with an amplitude of 10 Oe and a frequency of 1000 Hz. Reprinted with permission from ref 36. Copyright 2020 Elsevier.

differential magnetization on the temperature in an *ac* magnetic field. Previously,[35,41] we compared the dependence of the magnetic phase transitions on the temperature of $Ba_2Mg_2Fe_{12}O_{22}$ powder samples produced by the two techniques—sol–gel autocombustion and sonochemical co-precipitation, by monitoring the changes in the ac differential magnetization of the powder with the temperature being increased in an ac magnetic field of a frequency of 1000 Hz and an amplitude of 10 Oe. At 183 K, we observed a change for the sample prepared by autocombustion; for the sample produced by sonochemistry, a change took place at 196 K. Both of these changes are connected to a phase transformation from a ferromagnetic to a spiral magnetic moments ordering. At 40 and 30 K, transitions were also observed for the samples obtained, respectively, by autocombustion and co-precipitation. They are related to a spin reorientation to a longitudinal conical arrangement. The differing temperatures of these transformations in the two specimens are the result of the differing sizes and shapes of the particles and to their orientation in the applied magnetic field. As the particle size and thickness increase, the transition temperature of a proper screw to a collinear ferromagnetic spin ordering also increases from 195 to 225 K, but the one having to do with the transition from a conical to a proper screw spin ordering decreases from 30 to 23 K.[35]

The influence of the substitution of the magnetic cation (Ni^{2+}) with Zn^{2+}, which is diamagnetic, on the magnetic phase transitions in $Ba_{0.5}Sr_{1.5}Zn_{2-x}Ni_xFe_{12}O_{22}$ (x = 0.8, 1, 1.5) powder was reported by Koutzarova et al.[36] Figure 6 presents the temperature dependence of the differential susceptibility of $Ba_{0.5}Sr_{1.5}Zn_{2-x}Ni_xFe_{12}O_{22}$ (x = 0.8, 1, 1.5). The ac susceptibility's real part rises with the temperature; however, a sharp

rise is visible at about 225 K. We should stress here that no maximum of the real part of the ac susceptibility is seen at 300 K for the x = 0.8 composition, as opposed to the cases of the other two samples. Moreover, no maximum exists in this composition's imaginary part around 280−290 K. This suggests that the transition from a helicoidal to a ferromagnetic arrangement takes place at temperatures exceeding room temperature. At 10 and 148 K, one can see two maxima in the ac susceptibility curves' imaginary parts. The one 148 K is related to the magnetic phase transformation from a conical to a helicoidal magnetic moments ordering. For sample x = 1, where the Zn-to-Ni ratio is unity, at 177 K, one can see a weak maximum in the plot of the ac susceptibility's imaginary part, together with a maximum at 282 K; these are, respectively, the result of magnetic phase transformations from a conical to a helicoidal magnetic moment ordering and from a helicoidal to a ferrimagnetic magnetic moments ordering. In the case of the highest level of substitution (x = 1.5), one maximum is only seen at 284 K in the ac susceptibility's imaginary part; we assume that it arises from a magnetic phase transformation from a helicoidal to a ferrimagnetic magnetic moments ordering.

Khanduri et al.[47] studied the influence of the degree of Ba^{2+} cations substitution with Sr^{2+} cations in $Ba_{2-x}Sr_xMg_2Fe_{12}O_{22}$ (x = 0−1.5) on the magnetic phase transition temperature by measuring the magnetic susceptibility in an *ac* magnetic field of 1 kOe. They observed two magnetic phase transitions below the Curie temperature corresponding to a collinear ferrimag-netic−proper screw spin ordering transition in the temperature range of 260−390 K and from a proper screw to a longitudinal conical magnetic moments ordering transition in the range of 20−40 K. They found that the temperatures of these two

magnetic phase transitions increase with increasing the Sr concentration.

CONCLUSION

Knowledge of the ground magnetic state and the magnetic transitions in new materials make it possible to gain a new insight into the electronic properties of solids. This review is focused on the synthesis of and phase transitions in the polycrystalline hexagonal ferrites of the Y-type. The most successful routes of preparation of single-phase Y-type hexaferrites are presented, together with a discussion on the effect of the particular method chosen on the material's magnetic characteristics. For over 60 years, the effective mechanism for obtaining a pure hexaferrite phase, including Y-type in particular, has remained unclear; thus, further research efforts are needed in this direction in the future. The results of these studies will not only allow obtaining single-phase samples, but will also be relevant in studying the mechanism of substitution of Fe^{3+} with other cations, as well as the occupation of Me^{2+} positions by two different metal cations. In this regard, the impact of the substitution of nonmagnetic cations Me^{2+} (Zn^{2+}, Mg^{2+}) with magnetic ones and the possible preference of the substituting elements to enter particular cation sites is also considered. More details are given on the several single-phase multiferroics belonging to the Y-type, in which the electric polarization arises from the existence of conical magnetic moments ordering, so that one can manipulate the polarization up to room temperature by using relatively weak magnetic fields. A special emphasis is placed on the magnetic phase transitions related to the observation of magneto-electric coupling in single crystals and the manifestation of this effect through changes in the structural and magnetic properties of the powder material from this hexaferrite class. Future research should focus on the modulation of magneto-crystalline anisotropy, the spin-cone symmetry, and the magnetic ordering by way of Me^{2+} and Fe^{3+} substitution, especially for the $Ba_{2-x}Sr_xMe_2Fe_{12}O_{22}$ system, to view of enhancing the magneto-electric effect. Substitution of magnetic by nonmagnetic cations and vice versa should not be considered the only way of increasing the magnetic phase transition temperature, as the strong magneto-electric effect observed with the inclusion of a rare-earth element in the Y-type hexaferrite system may open new possibilities. Exploring the magnetic phase transition and the cation distribution is of great importance in preparing materials in which large ferroelectricity and strong ferromagnetism coexist.

AUTHOR INFORMATION

Corresponding Author

Tatyana Koutzarova − *Institute of Electronics, Bulgarian Academy of Sciences, 1784 Sofia, Bulgaria;* ⊙ orcid.org/0000-0002-5602-9019; Email: tanya@ie.bas.bg, tatyana_koutzarova@yahoo.com

Authors

Svetoslav Kolev − *Institute of Electronics, Bulgarian Academy of Sciences, 1784 Sofia, Bulgaria; Neofit Rilski South-Western University, 2700 Blagoevgrad, Bulgaria;* ⊙ orcid.org/0000-0003-4736-1631

Kiril Krezhov − *Institute of Electronics, Bulgarian Academy of Sciences, 1784 Sofia, Bulgaria*

Borislava Georgieva − *Institute of Electronics, Bulgarian Academy of Sciences, 1784 Sofia, Bulgaria;* ⊙ orcid.org/0000-0002-9529-3998

Complete contact information is available at:
https://pubs.acs.org/10.1021/acsomega.2c05689

Notes
The authors declare no competing financial interest.

Biographies
Tatyana Koutzarova is currently an associate professor and Head of Microwave Magnetics Laboratory of the Institute of Electronics, Bulgarian Academy of Sciences. Her research interests are in the field of magnetic oxide preparation of multiferroic materials, nanopowders, films, nanocomposites, and microwave absorbers.

Svetoslav Kolev is at present an associate professor at the Institute of Electronics, Bulgarian Academy of Sciences, and also at the Neofit Rilski South-Western University. His research interests are in the field of magnetic oxides preparation and investigation of multiferroic materials, nanopowders, thin and thick films, nanocomposites, and microwave absorbers.

Kiril Krezhov is currently a professor at the Institute of Electronics, Bulgarian Academy of Sciences. His research interests include the atomic structure of materials, crystallography, magnetism, nanomaterials, the interaction of neutrons and accelerated ions with the condensed matter as a means to change certain properties, and the use of elastic and inelastic neutron scattering techniques.

Borislava Georgieva is a Ph.D. student at the Microwave Magnetics Laboratory of the Institute of Electronics, Bulgarian Academy of Sciences. Her Ph.D. research deals with synthesis and structural and magnetic investigation of Y-type hexaferrite materials.

ACKNOWLEDGMENTS

REFERENCES

(1) Hill, N. A. Why are there so few magnetic ferroelectrics. *J. Phys. Chem. B* **2000**, *104*, 6694−6709.

(2) Hur, N.; Park, S.; Sharma, P. A.; Ahn, J. S.; Guha, S.; Cheong, S. W. Electric polarization reversal and memory in a multiferroic material induced by magnetic fields. *Nature* **2004**, *429*, 392−395.

(3) Hemberger, J.; Lunkenheimer, P.; Fichtl, R.; Krug von Nidda, H. A.; Tsurkan, V.; Loidl, A. Relaxor ferroelectricity and colossal magnetocapacitive coupling in ferromagnetic $CdCr_2S_4$. *Nature* **2005**, *434*, 364−367.

(4) Tokura, Y.; Seki, Sh. Multiferroics with spiral spin orders. *Adv. Mater.* **2010**, *22*, 1554−1565.

(5) Shen, S.; Chai, Y.; Sun, Y. Nonvolatile electric-field control of magnetization in a Y-type hexaferrite. *Sci. Rep.* **2015**, *5*, 8254.

(6) Cheong, S. W.; Mostovoy, M. Multiferroics: a magnetic twist for ferroelectricity. *Nat. Mater.* **2007**, *6*, 13−20.

(7) Chai, Y. S.; Kwon, S.; Chun, S. H.; Kim, I.; Jeon, B. G.; Kim, K. H.; Lee, S. Electrical control of large magnetization reversal in a helimagnet. *Nature Comm.* **2014**, *5*, 4208.

(8) Tan, G.; Chen, X. Synthesis, structures, and multiferroic properties of strontium hexaferrite ceramics. *J. Electron. Mater.* **2013**, *42*, 906−911.

(9) Kimura, T.; Lawes, G.; Ramirez, A. P. Electric polarization rotation in a hexaferrite with long-wavelength magnetic structures. *Phys. Rev. Lett.* **2005**, *94*, 137201.

(10) Utsumi, S.; Yoshiba, D.; Momozawa, N. Superexchange interactions of $(Ba_{1-x}Sr_x)_2Zn_2Fe_{12}O_{22}$ system studied by neutron diffraction. *J. Phys. Soc. Jpn.* **2007**, *76*, 034704.

(11) Pullar, R. C. Hexagonal ferrites: A review of the synthesis, properties and applications of hexaferrite ceramics. *Prog. Mater. Sci.* **2012**, *57*, 1191−1334.

(12) Taniguchi, K.; Abe, N.; Ohtani, S.; Umetsu, H.; Arima, T. Ferroelectric polarization reversal by a magnetic field in multiferroic Y-type hexaferrite $Ba_2Mg_2Fe_{12}O_{22}$. *Appl. Phys. Express* **2008**, *1*, 031301.

(13) Kouril, K.; Chlan, V.; Štepánková, H.; Telfah, A.; Novák, P.; Knížek, K.; Hiraoka, Y.; Kimura, T. Distribution of Zn in magnetoelectric Y-Type hexaferrite. *Acta Phys. Polym., A* **2010**, *118*, 732−733.

(14) Smit, J.; Wijn, H. P. J. *Ferrites*; Philips Technical Library: Eindhoven, 1959; p 150.

(15) Gorter, E. W. Saturation magnetization of some ferrimagnetic oxides with hexagonal crystal structures. *Proc. IEE - Part B: Radio and Electronic Engineering* **1957**, *104*, 255−260.

(16) Ishiwata, Sh.; Okuyama, D.; Kakurai, K.; Nishi, M.; Taguchi, Y.; Tokura, Y. Neutron diffraction studies on the multiferroic conical magnet $Ba_2Mg_2Fe_{12}O_{22}$. *Phys. Rev. B* **2010**, *81*, 174418.

(17) Momozawa, N.; Yamaguchi, Y.; Takei, H.; Mita, M. Magnetic structure of $(Ba_{1-x}Sr_x)_2Zn_2Fe_{12}O_{22}$ (x = 0−1.0). *J. Phys. Soc. Jpn.* **1985**, *54*, 771−780.

(18) Chai, Y S; Chun, S H; Haam, S Y; Oh, Y S; Kim, I.; Hoon Kim, K. Low-magnetic-field control of dielectric constant at room temperature realized in $Ba_{0.5}Sr_{1.5}Zn_2Fe_{12}O_{22}$. *New J. Phys.* **2009**, *11*, 073030.

(19) Ishiwata, Sh.; Taguchi, Y.; Murakawa, H.; Onose, Y.; Tokura, Y. Low-magnetic-field control of electric polarization vector in a helimagnet. *Science* **2008**, *319*, 1643−1646.

(20) Zhuravlev, V. A.; Wagner, D. V.; Dotsenko, O. A.; Kareva, K. V.; Zhuravlyova, E. V.; Chervinskaya, A. S.; Kuleshov, G. E.; Suraev, A. S. Static and Dynamic Magnetic Properties of Polycrystalline Hexaferrites of the $Ba_2Ni_{2-x}Cu_xFe_{12}O_{22}$ System. *Electronics* **2022**, *11*, 2759.

(21) Abdullah, Md. F.; Pal, P.; Chandrakanta, K.; Jena, R.; Devi, S.; Yadav, C. S.; Singh, A. K. Enhanced magnetic and room temperature intrinsic magnetodielectric effect in Mn modified $Ba_2Mg_2Fe_{12}O_{22}$ Y-type hexaferrite. *J. Phys.: Condens. Matter.* **2020**, *32*, 135701.

(22) Abdullah, Md. F.; Devi, S.; Jena, R.; Chandrakanta, K.; Pal, P.; Yadav, C. S.; Singh, A. K. Evidence of room temperature magnetodielectric and cluster glass behavior of Sr substituted Y-type $Ba_2Mg_2Fe_{11.48}Mn_{0.52}O_{22}$ hexaferrite. *J. Magn. Magn. Mater.* **2022**, *552*, 169191.

(23) Fujii, S.; Nishijima, K.; Satoh, H.; Yamamoto, S. Co2-Y ferrite modified by CuO addition applied to a terrestrial broadcasting antenna. *J. Magn. Magn. Mater.* **2015**, *379*, 256−259.

(24) Li, Z. W.; Chua, M. J.; Yang, Z. H. Studies of static, high-frequency and electromagnetic attenuation properties for Y-type hexaferrites $Ba_2Cu_xZn_{2-x}Fe_{12}O_{22}$ and their composites. *J. Magn. Magn. Mater.* **2015**, *382*, 134−141.

(25) Wang, Y.; Zhang, Sh.; Zhu, W. K.; Ling, L.; Zhang, L.; Qu, Z.; Pi; Tong, W.; Tian; Zhang, Y. Nonzero electric polarization and four magnetoelectric states at zero magnetic field in Cr-doped Y-type hexaferrite. *J. Appl. Phys.* **2017**, *110*, 262901.

(26) Yang, Y.; Jiang, K; Wu, Q.; Ge, H. Large magnetoelectric coupling in a Y-type hexaferrite. *Phys. Status Solidi B* **2020**, *257*, 1900257.

(27) Rhee, Ch. H.; Lim, J. T.; Kim, Ch. S.; Kim, S. B. Neutron diffraction and magnetic properties of $Ba_2Co_2Fe_{12}O_{22}$: Co_2Y. *J. Korean Phys. Soc.* **2013**, *62*, 1919−1921.

(28) Wang, F.; Zou, T.; Yan, L.; Liu, Y.; Sun, Y. Low magnetic field reversal of electric polarization in a Y-type hexaferrite. *Appl. Phys. Lett.* **2012**, *100*, 122901.

(29) Gao, Y.; Wu, Q.; Song, J.; Man, Q. Achieving broad absorption bandwidth of $Ba_2Co_2Fe_{12}O_{22}$ ferrites by adjusting the sintering temperature. *J. Magn. Magn. Mater.* **2022**, *554*, 169312.

(30) Xu, W.; Wang, Zh.; Yang, J.; Bai, W.; Zhang, Y.; Tang, X. Magnetic and dielectric properties in multiferroic Y-type hexaferrite. *Mol. Cryst. Liq. Cryst.* **2014**, *603*, 235−239.

(31) Georgieva, B.; Kolev, S.; Krezhov, K.; Ghelev, Ch.; Kovacheva, D.; Tran, L. M.; Babij, M.; Zaleski, A.; Vertruyen, B.; Closset, R.; Koutzarova, T. Magnetic phase transitions in $Ba_{0.5}Sr_{1.5}Zn_2Fe_{11.92}Al_{0.08}O_{22}$ hexaferrites. *J. Phys. Conf. Ser.* **2021**, *1762*, 012034.

(32) Georgieva, B.; Kolev, S.; Krezhov, K.; Ghelev, Ch.; Kovacheva, D.; Tran, L. M.; Babij, M.; Zaleski, A.; Vertruyen, B.; Closset, R.; Koutzarova, T. Effect of Ni and Al substitution on the magnetic properties of Y-type hexaferrite $Ba_{0.5}Sr_{1.5}Zn_{0.5}Ni_{1.5}Fe_{11.92}Al_{0.08}O_{22}$ powders. *J. Phys. Conf. Ser.* **2021**, *1859*, 012067.

(33) Koutzarova, T.; Kolev, S.; Nedkov, I.; Krezhov, K.; Kovacheva, D.; Blagoev, B.; Ghelev, C.; Henrist, C.; Cloots, R.; Zaleski, A. Magnetic properties of nanosized $Ba_2Mg_2Fe_{12}O_{22}$ powders obtained by auto-combustion. *J. Supercond. Nov. Magn.* **2012**, *25*, 2631−2635.

(34) Ahmad, B.; Ashiq, M. N.; Khan, M. S.; Osada, M.; Najam-Ul-Haq, M.; Ali, I. Elucidation of structure and conduction mechanism in Nd-Mn substituted Y-type strontium hexaferrites. *J. Alloy. Compd.* **2017**, *723*, 9−16.

(35) Georgieva, B.; Krezhov, K.; Kolev, S.; Ghelev, Ch.; Kovacheva, D.; Fabian, M.; Svab, E.; Koutzarova, T. Characterization of Y-type hexaferrite $Ba_2Mg_2Fe_{12}O_{22}$ powders. *IEEE Xplore* **2017**, 39−44.

(36) Koutzarova, T.; Kolev, S.; Krezhov, K.; Georgieva, B.; Ghelev, Ch.; Kovacheva, D.; Vertruyen, B.; Closset, R.; Tran, L. M.; Babij, M.; Zaleski, A. J. Ni-substitution effect on the properties of $Ba_{0.5}Sr_{1.5}Zn_{2-x}Ni_xFe_{12}O_{22}$ powders. *J. Magn. Magn. Mater.* **2020**, *505*, 166725.

(37) Daigle, A.; DuPre', E.; Geiler, A.; Chen, Y.; Parimi, P. V.; Vittoria, C.; Harris, V. G. Preparation and characterization of pure-phase Co_2Y ferrite powders via a scalable aqueous coprecipitation method. *J. Am. Ceram. Soc.* **2010**, *93*, 2994−2997.

(38) Chen, W.; Dai, J.; Xia, J.; Ding, Y.; Hu, Z. Technological conditions and magnetic properties of Y-type hexaferrite prepared by chemical co-precipitation method. *Adv. Mater. Res.* **2011**, *412*, 146−149.

(39) Hsiang, H.-I.; Yao, R.-Q. Hexagonal ferrite powder synthesis using chemical coprecipitation. *Mater. Chem. Phys.* **2007**, *104*, 1−4.

(40) Lehlooh, A. F.; Alghazo, R.; Rawwagah, F.; Hammoudeh, A.; Mahmood, S. Mössbauer spectroscopy study of Y-type hexaferrite $(Ba_2Co_2Fe_{12}O_{22})$ prepared by the co-precipitation method. *Hyperfine Interact.* **2020**, *241*, 12.

(41) Koutzarova, T.; Kolev, S.; Nedkov, I.; Krezhov, K.; Kovacheva, D.; Ghelev, Ch.; Vertruyen, B.; Henrist, C.; Cloots, R. Study of quasi-monophase Y-type hexaferrite $Ba_2Mg_2Fe_{12}O_{22}$ powder. *Micro and Nanosystems* **2014**, *6*, 14−20.

(42) Koutzarova, T.; Kolev, S.; Krezhov, K.; Georgieva, B.; Kovacheva, D.; Ghelev, Ch.; Vertruyen, B.; Boschini, F.; Mahmoud, A.; Tran, L. M.; Zaleski, A. Study of the structural and magnetic properties of co-substituted $Ba_2Mg_2Fe_{12}O_{22}$ hexaferrites synthesized by sonochemical co-precipitation. *Materials* **2019**, *12*, 1414.

(43) Georgieva, B. V.; Koutzarova, T. I.; Kolev, S. M.; Ghelev, Ch. G.; Vertruyen, B.; Closset, R.; Cloots, R.; Zaleski, A. Study of quasi-monophase Y-type hexaferrite $Ba_{0.5}Sr_{1.5}Zn_2Al_{0.08}Fe_{11.92}O_{22}$ powders. *Bulg. Chem. Commun.* **2016**, *48* (G), 147−150.

(44) Georgieva, B.; Kolev, S.; Krezhov, K.; Ghelev, Ch.; Kovacheva, D.; Vertruyen, B.; Closset, R.; Tran, L. M.; Babij, M.; Zaleski, A. J.; Koutzarova, T. Structural and magnetic characterization of Y-type hexaferrite powders prepared by sol-gel auto-combustion and sonochemistry. *J. Magn. Magn. Mater.* **2019**, *477*, 131−135.

(45) Georgieva, B.; Kolev, S.; Ghelev, Ch.; Koutzarova, T.; Kovacheva, D.; Vertruyen, B.; Closset, R. A Comparative study of the morphology of Y-type hexaferrite powders obtained by sol-gel auto-combustion and ultrasonic co-precipitation. In *Advanced Nano-technologies for Detection and Defence against CBRN Agents*; Petkov, P., Tsiulyanu, D., Popov, C., Kulisch, W., Eds.; NATO Science for Peace and Security Series B: Physics and Biophysics; Springer: Dordrecht, 2018; pp 31−36.

(46) Fujii, S.; Nishijima, K.; Satoh, H.; Yamamoto, S. Co2-Y ferrite modified by CuO addition applied to a terrestrial broadcasting antenna. *J. Magn. Magn. Mater.* **2015**, *379*, 256−259.

(47) Khanduri, H.; Chandra Dimri, M.; Kooskora, H.; Heinmaa, I.; Viola, G.; Ning, H.; Reece, M. J.; Krustok, J.; Stern, R. Structural, dielectric, magnetic, and nuclear magnetic resonance studies of multiferroic Y-type hexaferrites. *J. Appl. Phys.* **2012**, *112*, 073903.

(48) Georgieva, B.; Kolev, S.; Ghelev, Ch.; Krezhov, K.; Kovacheva, D.; Vertruyen, B.; Closset, R.; Tran, L. M.; Babij, M.; Zaleski, A.; Koutzarova, T. Effect of cation substitutions in Y-type $Ba_{0.5}Sr_{1.5}Me_2Fe_{12}O_{22}$ hexaferrites on the magnetic phase transitions. *J. Phys. Conf. Ser.* **2022**, *2240*, 012023.

(49) Novák, P.; Knížek, K.; Rusz, J. Magnetism in the magneto-electric hexaferrite system $(Ba_{1-x}Sr_x)_2Zn_2Fe_{12}O_{22}$. *Phys. Rev. B* **2007**, *76*, 024432.

(50) Zhang, M.; Dai, J.; Yin, L.; Kong, X.; Liu, Q.; Zi, Z.; Sun, Y. Mg doping effect on the magnetic properties of Y-type hexaferrite $Ba_{0.5}Sr_{1.5}Zn_{2-x}Mg_xFe_{12}O_{22}$. *J. Alloys Compd.* **2016**, *689*, 75−80.

(51) Zhang, M.; Yin, L.; Liu, Q.; Kong, X.; Zi, Z.; Dai, J.; Sun, Y. Magnetic properties and magnetodielectric effect in Y-type hexaferrite $Ba_{0.5}Sr_{1.5}Zn_{2-x}Mg_xFe_{11}AlO_{22}$. *J. Alloys Compd.* **2017**, *725*, 1252−1258.

(52) Kim, J.; Choi, H.; Kim, Ch. S. Magnetic properties of polycrystalline Y-type hexaferrite $Ba_{2-x}Sr_xNi_2(Fe_{1-y}Al_y)_{12}O_{22}$ using Mössbauer spectroscopy. *AIP Advances* **2020**, *10*, 015204.

(53) Lim, J. T.; Kim, Ch. M.; Lee, B. W.; Kim, C. S. Investigation of magnetic properties of non-magnetic ion (Al, Ga, In) doped $Ba_2Mg_{0.5}Co_{1.5}Fe_{12}O_{22}$. *J. Appl. Phys.* **2012**, *111*, 07A518.

(54) Kim, C. M.; Rhee, Ch. H.; Kim, Ch. S. Preference for Fe in Zn-doped Y-type barium hexaferrite. *IEEE Trans. Magn.* **2012**, *48*, 3414−3417.

(55) Lim, J. T.; Kim, Ch. S. Investigation of magnetic properties of Zn doped Y-type barium ferrite. *IEEE Trans. Magn.* **2013**, *49*, 4192−4195.

(56) Behera, P.; Ravi, S. Magnetic and dielectric spectroscopic studies in Zn substituted Y-type barium hexaferrite. *J. Alloy. Compd.* **2018**, *767*, 712−723.

(57) Behera, P.; Ravi, S. Impedance spectroscopy and magnetic properties of Mg doped Y-type barium hexaferrite. *J. Mater. Sci.: Mater. Electron.* **2018**, *29*, 20206−20215.

(58) Wang, G.; Cao, S.; Cao, Y.; Hu, S.; Wang, X.; Feng, Z.; Kang, B.; Chai, Y.; Zhang, J.; Ren, W. Magnetic field controllable electric polarization in Y-type hexaferrite $Ba_{0.5}Sr_{1.5}Co_2Fe_{12}O_{22}$. *J. Appl. Phys.* **2015**, *118*, 094102.